Earth and Planetary Science Letters 426 (2015) 225–234

Contents lists available at ScienceDirect

Earth and Planetary Science Letters

www.elsevier.com/locate/epsl

Tracing chlorine sources of thermal and mineral springs along and across the Cascade Range using halogen concentrations and chlorine isotope compositions

Jeffrey T. Cullen [a,*], Jaime D. Barnes [a], Shaul Hurwitz [b], William P. Leeman [c,1]

[a] Department of Geological Sciences, University of Texas, Austin, TX 78712, USA
[b] U.S. Geological Survey MS #439, 435 Middlefield Rd., Menlo Park, CA 94025, USA
[c] Department of Earth Science, MS-126, Rice University, Houston, TX 77005, USA

ARTICLE INFO

Article history:
Received 24 February 2015
Received in revised form 24 June 2015
Accepted 25 June 2015
Available online xxxx
Editor: T.A. Mather

Keywords:
halogen
stable isotope
chlorine isotope
Cascade Range
thermal springs
hydrothermal

ABSTRACT

In order to provide constraints on the sources of chlorine in spring waters associated with arc volcanism, the major/minor element concentrations and stable isotope compositions of chlorine, oxygen, and hydrogen were measured in 28 thermal and mineral springs along the Cascade Range in northwestern USA. Chloride concentrations in the springs range from 64 to 19,000 mg/L and δ^{37}Cl values range from +0.2‰ to +1.9‰ (average = +1.0 ± 0.4‰), with no systematic variation along or across the arc, nor correlations with their presumed underlying basement lithologies. Additionally, nine geochemically well-characterized lavas from across the Mt. St. Helens/Mt. Adams region of the Cascade Range (Leeman et al., 2004, 2005) were analyzed for their halogen concentrations and Cl isotope compositions. In the arc lavas, Cl and Br concentrations from the volcanic front are higher than in lavas from the forearc and backarc. F and I concentrations progressively decrease from forearc to backarc, similar to the trend documented for B in most arcs. δ^{37}Cl values of the lavas range from −0.1 to +0.8‰ (average = +0.4 ± 0.3‰). Our results suggest that the predominantly positive δ^{37}Cl values observed in the springs are consistent with water interaction with underlying ^{37}Cl-enriched basalt and/or altered oceanic crust, thereby making thermal spring waters a reasonable proxy for the Cl isotope compositions of associated volcanic rocks in the Cascades. However, waters with δ^{37}Cl values > + 1.0‰ also suggest additional contributions of chlorine degassed from cooling magmas due to subsurface vapor–liquid HCl fractionation in which Cl is lost to the aqueous fluid phase and ^{37}Cl is concentrated in the ascending magmatic HCl vapor. Future work is necessary to better constrain Cl isotope behavior during volcanic degassing and fluid–rock interaction in order to improve volatile flux estimates through subduction zones.

© 2015 Elsevier B.V. All rights reserved.

1. Introduction

Volatiles and fluid mobile elements (e.g., Cl, Br, B, F, S, Pb, As) are liberated from subducted oceanic slabs as a consequence of metamorphic dehydration reactions and returned to the Earth's surface (e.g., Bebout, 2007; Manning, 2004). Understanding the behavior of volatiles in subduction zones is important for quantifying global element fluxes. Cascadia is regarded as the warmest subduction zone (Syracuse et al., 2010) and thermal and petrologic models predict that the slab is strongly dehydrated before it reaches depths of magma genesis (e.g., van Keken et al., 2011). Seismic images suggest extensive serpentinization of the mantle wedge beneath the Cascadia forearc due to upward migration of slab-derived fluids (Bostock et al., 2002; Brocher et al., 2003).

Quantifying the concentrations of magmatic volatiles dissolved in groundwater and discharged through thermal springs allows for a more comprehensive estimate of the overall volatile fluxes through subduction zones (which rarely include volatile inventories in thermal springs), assessment of processes that control the abundance of volatiles liberated from the slab, and monitoring of volcanic activity due to fluctuations in shallow magmatic inputs. However, a major challenge with this approach is distinguishing magmatic versus non-magmatic volatile components in the springs. In the central Oregon Cascade Range, halogen concentrations and ratios of the radioisotopes ^{36}Cl and ^{129}I (Hurwitz et al., 2005), carbon isotopes (Evans et al., 2004; James et al., 1999),

* Corresponding author.
E-mail address: jcullen@utexas.edu (J.T. Cullen).
[1] Now at 642 Cumbre Vista, Santa Fe, NM 87501, USA.

http://dx.doi.org/10.1016/j.epsl.2015.06.052
0012-821X/© 2015 Elsevier B.V. All rights reserved.

and helium isotopes (Evans et al., 2004) of thermal spring waters suggest that most of the halogens are magmatically derived. In contrast, Mariner et al. (2003) argue that Cl (and excess nitrogen) in central Cascade thermal springs are mainly sourced from underlying sedimentary units. It remains uncertain what relative chloride contributions are derived from [1] seawater/seaspray, [2] underlying sedimentary units (including connate water), [3] magma, and/or [4] Cl extracted from subsurface volcanic units via water–rock interactions.

Chloride, and to a lesser extent, Br, F, and I are often used as fluid tracers in subduction zones and for interpreting the extent and style of magma degassing (e.g., Fehn, 2012; Kendrick et al., 2012; Straub and Layne, 2003; Villemant and Boudon, 1999; Villemant et al., 2005). Stable Cl isotope ratios also have been used to trace sources through subduction zones (e.g., Barnes et al., 2008; Barnes et al., 2009; Chiaradia et al., 2014; Li et al., 2015). However, apart from the study of Li et al. (2015), all of these isotopic studies have focused on volcanic outputs in the form of gas and lava, and not addressed sources of Cl in thermal waters.

Reported δ^{37}Cl values of thermal waters are few and the available data cluster near 0‰: Indonesian volcanic springs (−0.3 to +0.4‰; Eggenkamp, 1994), Icelandic thermal waters (−0.3 to +0.3‰; Barnes and Stefansson, 2012), Yellowstone springs (−0.1‰ to +0.4‰; Zhang et al., 2004), Taupo Volcanic Zone (−0.8‰ to +0.7‰; Bernal et al., 2014), and Soufrière in Guadeloupe and Montagne Pelée in Martinique in the Lesser Antilles (−0.65‰ to +0.12‰; Li et al., 2015). None of these studies report halogen concentrations or Cl isotope compositions for the associated volcanic rocks, thus making it difficult to ascertain the extent to which the host rocks may control the chemistries of the thermal springs.

Here we report chemical and stable chlorine isotope compositions of waters from 28 thermal (≥8.3 °C above the mean ambient air temperature) and/or mineral springs (containing ≥500 mg/L total dissolved solids (TDS)) in the Cascade Range (Fig. 1). Water sample sites are distributed over 900 km along strike, and cover the forearc, volcanic front, and backarc regions. We also report halogen concentrations and the Cl isotope composition of nine well-characterized lavas (8 basalts and 1 dacite) from the Columbia Transect in southwest Washington (Fig. 1) (Leeman et al., 2004, 2005). The new data are used to assess the sources, spatial variability, and isotopic composition of chloride in the springs along and across the arc.

2. Geologic overview the of Cascade Range and associated mineral and thermal springs

The Cascade Range stretches approximately 1300 km from northern California to southern British Columbia, and is associated with the eastward subduction of the Juan de Fuca, Gorda, and Explorer plates beneath North America (Fig. 1). Near the active trench, the subducting plates are relatively young (2–28 my) (Wilson, 1988), resulting in a warm subduction zone compared to most other volcanic arcs (Leeman et al., 2005; Syracuse et al., 2010). The Cascade Range comprises volcanic deposits, mainly basalt to dacite in composition, of Eocene–Quaternary age with cumulate thickness up to several kilometers across the older western and more recent High Cascades sectors (Hildreth, 2007). The underlying basement includes marine shales, limestones and sandstones, Paleozoic accreted oceanic terranes of OIB- and MORB-like basalt, and tectonic slivers of serpentinized peridotites (Wells et al., 2014).

Many previous studies of thermal springs in the Cascade Range were largely motivated by the region's geothermal potential (e.g., Ingebritsen et al., 1989, 1991; Mariner et al., 1990). Recent work has focused on Cl flux, and its source(s), because Cl discharge is used as a proxy for heat, and thus magmatic activity (e.g., Evans et al., 2004; Hurwitz et al., 2005). Cascade Range thermal waters are predominantly meteoric in origin, largely Na–Cl/Ca–Na–Cl type, and have a large range in temperature, discharge rate, and composition irrespective of their regional geographic locations (e.g., Ingebritsen et al., 1991).

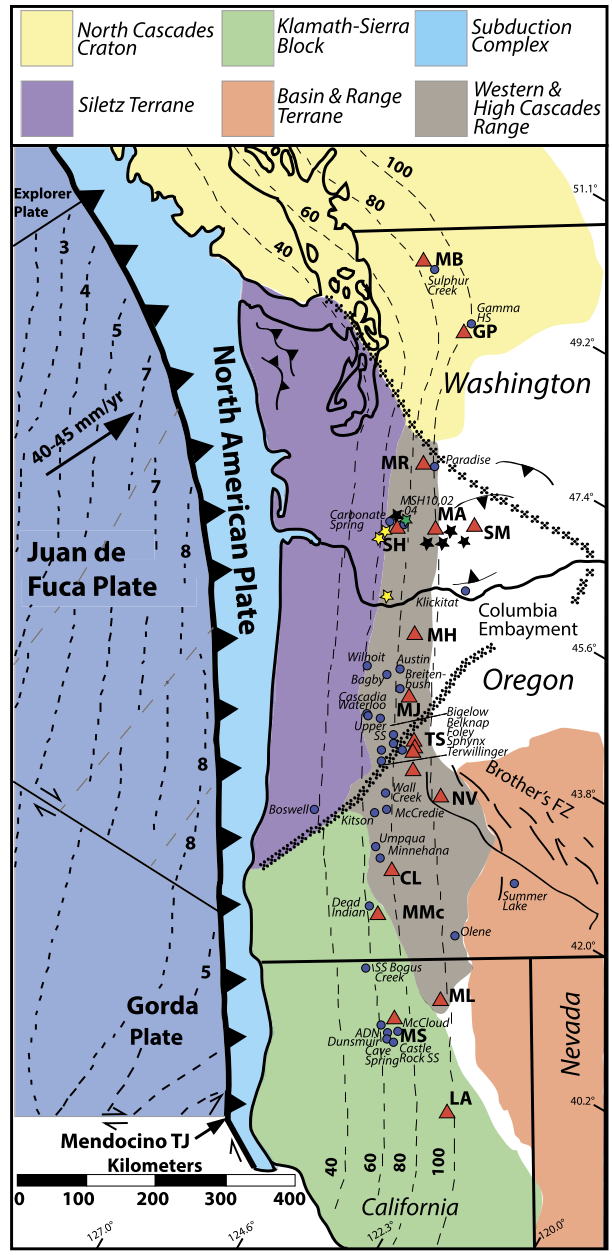

Fig. 1. Map of isotopically distinguishable terranes along the Cascade volcanic arc as outlined by Schmidt et al. (2008). Dashed contours show approximate depths to the slab in km (McCrory et al., 2004). Dashed lines on oceanic plates are magnetic anomalies (Wilson, 1988). Major volcanoes are illustrated as red triangles: (LA) Lassen, (MS) Mt. Shasta, (ML) Medicine Lake, (MMc) Mt. McLaughlin, (CL) Crater Lake, (NV) Newberry Volcano, (TS) Three Sisters, (MJ) Mt. Jefferson, (MH) Mt. Hood, (SH) Mt. St. Helens, (MA) Mt. Adams, (SM) Simcoe, (MR) Mt. Rainer, (GP) Glacier Peak, (MB) Mt. Baker, (MG), Mt. Garibaldi, (MC). Mt. Cayley, (MM) Mt. Meager. Springs sampled as part of this study are labeled and indicated by blue circles. Columbia Transect lavas are indicted by yellow stars (Group 2 basalts), black stars (Group 1 basalts) and green star (high crustal melt dacite) in SW Washington (Leeman et al., 2004, 2005). Modified from Schmidt et al. (2008). (For interpretation of the references to color in this figure legend, the reader is referred to the web version of this article.)

3. Sampling methods and analytical techniques

Twenty-eight spring water samples were collected during the summer of 2012 (Fig. 1). Waters discharging through pools were collected using Tygon tubing lowered into the pool and attached to a peristaltic pump to minimize contamination. In cases where multiple discharge points for a single spring were present, the hottest water was collected. Samples were filtered through a 0.45 µm membrane and collected in polyethylene bottles for anion, cation, alkalinity, and chlorine isotope analyses. Samples used for cation analysis were acidified in the field with 18N HNO_3 to a pH of ∼2. A 15 cm^3 glass bottle fitted with a Teflon cap was filled for hydrogen and oxygen isotope analysis.

Cation concentrations were measured on an Agilent 7500ce Quadrapole ICP-MS in the Department of Geological Sciences, University of Texas at Austin. Multiple dilutions of NIST 1643e were used as primary reference standard in the analysis. Analytical uncertainties are <3% relative. Concentrations of major anions (Cl^-, SO_4^{2-}, Br^-, F^-) were determined using a Dionex ion chromatograph at the U.S. Geological Survey in Menlo Park, CA with analytical errors of <3% for Cl^-, F^-, and SO_4^{2-} and <5% for Br^-. Iodine concentrations were determined with a PerkinElmer NexION 300 inductively coupled plasma mass spectrometer (ICP-MS) at the USGS in Menlo Park using established methods (Schnetger and Muramatsu, 1996); analytical errors are 20%. Total alkalinity was measured by acid titration within 14 days of sampling on a METROHM 702 SM Titrino auto-titrator.

Oxygen isotope analyses were obtained by continuous-flow mass spectrometry on one milliliter water samples following equilibration with CO_2 for 24 hours at 25 °C in septum-capped glass vials. Internal lab standards were calibrated by applying a stretching factor that resulted in a value of −55.5‰ for SLAP (Standard Light Antarctic Precipitation) relative to SMOW (Standard Mean Ocean Water). Standard error is ±0.1‰ (1σ). For hydrogen isotope analysis, 10 µL water samples were reduced to H_2 gas on glassy carbon using a TCEA (Thermo Conversion Elemental Analyzer) coupled to a ThermoElectron MAT 253. Errors on δD values are ±2‰ (1σ). Both δD and δ^{18}O values are reported in standard per mil (‰) notation relative to SMOW.

Water samples were analyzed for chlorine isotope composition following the procedures of Eggenkamp (1994). Chlorine was precipitated as AgCl by the addition of $AgNO_3$ and subsequently converted to CH_3Cl by reaction with CH_3I. δ^{37}Cl values were measured on a ThermoElectron MAT 253 mass spectrometer and are reported in standard per mil notation vs. SMOC (Standard Mean Ocean Chloride; $\delta^{37}Cl_{SMOC} = 0‰$). Analytical precision is ±0.2‰, based on long-term analyses of three in-house seawater standards and one in-house rock standard. Eight of the spring samples were reproduced for δ^{37}Cl values; five of the eight reproduced within analytical error (±0.2‰). The reason for the poor reproducibility for the other three samples is unclear, but may be due to incomplete removal of sulfur resulting in incomplete extraction of Cl (e.g., Sharp et al., 2010).

Halogen concentrations and Cl isotope compositions were measured in nine lavas from an across-arc segment in southern Washington (Fig. 1); these samples were previously analyzed for major and trace element and Sr–Pb–Nd–B isotope compositions by Leeman et al. (2004, 2005). Halogens were extracted from the rock powders using the pyrohydrolysis technique of Schnetger and Muramatsu (1996). Released halogens and water vapor were collected as condensates in a trapping solution of NaOH (0.05N) and Na_2SO_3 (0.005N). F concentrations were determined by ion chromatography. Cl^-, Br^-, and I^- concentrations were determined using a ThermoFinnigan Element 2 ICP-MS at the University of Bremen. Limits of detection are 16, 0.4, and 0.06 µg/L, respectively. δ^{37}Cl values of the rock powders were determined using the condensate solution.

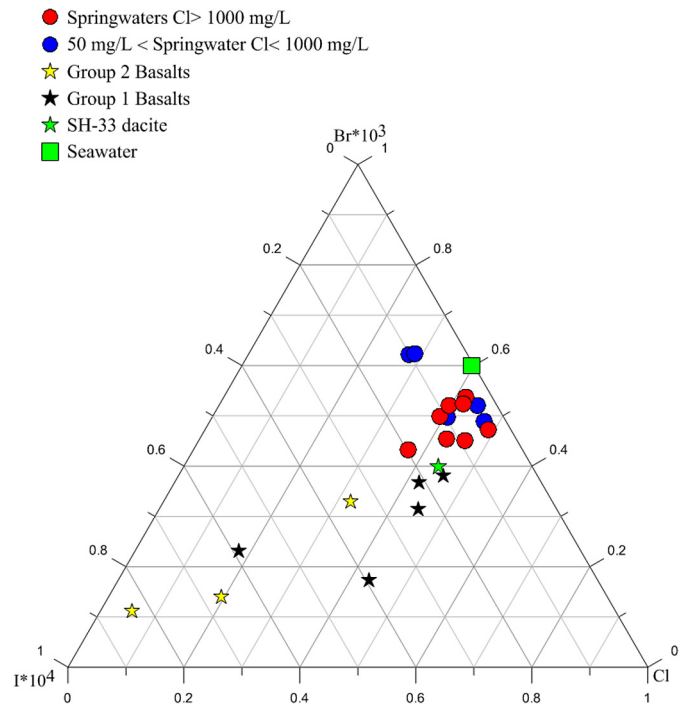

Fig. 2. Ternary diagram of Br, I, and Cl molar concentrations of spring waters and lavas, plotted as equivalents.

4. Results

4.1. Chemistry of the thermal and mineral spring waters

The concentrations and compositions of major cations in the spring waters are highly variable (Table 1). Chloride is the major anion in most spring waters (Table 1). We note that for this study only samples with Cl >50 mg/L are considered so as to eliminate samples strongly diluted by meteoric water. However, bicarbonate is the dominant anion in Castle Rock Soda Spring (near Mt. Shasta in Northern California) and in Dead Indian Soda Spring (Southern Oregon), and sulfate is a significant component in Paradise Warm Spring (near Mt. Rainier in Washington) (Fig. 1; Table 1). Maximum Cl^-, Br^-, F^-, and I^- concentrations in the springs are 19,000 mg/L, 50 mg/L, 4.2 mg/L and 3600 µg/L, respectively (Fig. 2).

4.2. O, H, and Cl Stable Isotopes

δD and δ^{18}O values range from −120‰ to −15‰ and from −13.6‰ to −2.3‰, respectively (Table 1; Fig. 3A). Thermal water compositions generally plot to the right of the global meteoric water line (GMWL), likely reflecting isotopic shifts due to water–rock interaction and/or boiling and evaporation from thermal pools. δ^{18}O values of the spring waters are loosely correlated with Cl concentrations (Fig. 3B). Chlorine isotope values of the samples range from +0.2‰ to +1.9‰ (average = +1.0‰ ± 0.4‰; median = +0.9‰). There is no significant correlation between δ^{37}Cl values and either Cl concentrations, δ^{18}O values, or temperature (Fig. 4). Also, there is no apparent relationship between the δ^{37}Cl values of the thermal springs and either elevation, along-arc location, or the nature of the underlying basement terrane (Fig. 5).

4.3. Columbia transect volcanic rocks

The eight representative basalts and one dacite lava from southwest Washington are of Quaternary–Recent age with no apparent

Table 1
Location, sampling temperature, and major geochemical data from the thermal spring waters analyzed. Concentrations are in mg/L with the exception of I in μg/L.

Spring name	Location	Elevation (m)	T (°C)	pH	B	Na	Mg	Si	K	Ca	Fe	HCO_3[a]	Cl	Br	F	I	SO_4	$\delta^{37}Cl$[b]	$\delta^{18}O$	δD
Boswell	N 43.642 W 123.298	93	14.2	8.6	6.8	3922	0.4	b.d.l	11	6890	0.04	27	19 000	50	< 0.1	3600	<5	0.5, 0.7	−2.3	−15
SS Bogus Creek	N 41.921 W 122.371	790	23.2	6.6	n.d.	n.d.	n.d.	n.d.	n.d.	n.d.	n.d.	n.d.	4150	5.0	<0.1	n.d.	n.d.	1.0	n.d.	n.d.
Upper Soda	N 44.405 W 122.285	425	12.2	6.1	n.d.	n.d.	n.d.	n.d.	n.d.	n.d.	n.d.	n.d.	3750	8.0	1.0	n.d.	n.d.	1.1	n.d.	n.d.
Umpqua	N 43.297 W 122.355	900	43.5	6.1	40.8	2244	41	38	63	347	1.92	1308	3400	7.5	0.9	240	190	0.3	−12.0	−101
Kitson	N 43.690 W 122.375	481	39.2	7.5	19.7	1189	2	18	21	601	0.01	30	2800	6.1	2.0	80	165	1.9	−11.9	−94
Cascadia	N 44.399 W 122.480	250	15.7	6.1	n.d.	n.d.	n.d.	n.d.	n.d.	n.d.	n.d.	n.d.	2675	9.0	1.0	n.d.	n.d.	0.5, 0.8	n.d.	n.d.
Wilhoit	N 45.052 W 122.568	232	10.7	6.2	n.d.	n.d.	n.d.	n.d.	n.d.	n.d.	n.d.	n.d.	2580	4.5	1.0	n.d.	n.d.	0.3, 1.1	n.d.	n.d.
McCredie	N 43.706 W 122.288	606	71.5	7.2	17.9	984	0.9	31	24	474	0.01	24	2200	5.3	2.6	222	250	0.0, 1.2	−12.4	−96
Waterloo	N 44.496 W 122.480	375	15.4	6.1	n.d.	n.d.	n.d.	n.d.	n.d.	n.d.	n.d.	n.d.	1645	5.0	1.0	n.d.	n.d.	0.6	n.d.	n.d.
Foley	N 44.154 W 122.098	590	79.2	6.2	8.5	531	0.1	28	9	514	0.01	22	1360	3.9	0.8	134	550	1.4	−11.6	−91
Belknap	N 44.239 W 122.059	566	86.5	7.5	5.6	634	0.9	32	16	191	0.03	20	1320	3.9	1.2	97	170	0.8	−11.4	−95
Bigelow	N 44.194 W 122.051	508	36.3	6.9	6.3	662	0.3	41	16	219	0.02	24	1240	3.6	1.5	48	144	1.0	−11.8	−99
Breitenbush	N 44.781 W 121.976	681	66.5	7.6	3.9	681	0.9	69	30	101	0.07	135	1100	3.1	3.5	53	132	0.9	−12.3	−102
Castle Rock SS	N 41.149 W 122.307	615	14.4	6.5	n.d.	n.d.	n.d.	n.d.	n.d.	n.d.	n.d.	n.d.	1020	2.9	0.4	n.d.	n.d.	1.3	n.d.	n.d.
Terwillinger	N 44.083 W 122.240	620	43.8	8.4	5.2	389	0.1	21	6	212	0.01	24	800	2.1	0.9	21	260	0.9, 0.7	−12.1	−92
Gamma Spring	N 48.153 W 121.063	1505	65.2	6.1	n.d.	n.d.	n.d.	n.d.	n.d.	n.d.	n.d.	n.d.	740	n.d.	n.d.	n.d.	n.d.	1.8	n.d.	n.d.
Wall Creek	N 43.807 W 122.311	653	38.3	7.8	6.5	331	0.2	29	9	113	0.03	43	600	1.4	4.2	17	147	1.1	−12.7	−96
Austin	N 45.019 W 122.000	518	86.5	7.5	2.6	300	0.1	38	7	37	0.01	56	400	1.1	1.3	34	138	1.5	−12.4	−100
Upper Dunsmuir	N 41.222 W 122.277	714	12.3	5.9	n.d.	n.d.	n.d.	n.d.	n.d.	n.d.	n.d.	n.d.	340	1.0	0.1	n.d.	n.d.	0.7, 0.7	n.d.	n.d.
Cave Spring	N 41.228 W 122.277	730	11.9	6.0	n.d.	n.d.	n.d.	n.d.	n.d.	n.d.	n.d.	n.d.	370	1.0	0.2	n.d.	n.d.	1.2, 1.4	n.d.	n.d.
Dead Indian	N 42.333 W 122.450	850	14.1	$6.0	n.d.	n.d.	n.d.	n.d.	n.d.	n.d.	n.d.	n.d.	364	0.3	0.1	n.d.	n.d.	0.3, 1.5	n.d.	n.d.
Summer Lake 1	N 42.725 W 120.647	1300	48	8.3	7.3	453	0.1	41	6	2	0.01	529	336	1.7	2.0	44	56	0.9	−13.4	−113
MSH10-03	N 46.21 W 122.19	1520	n.d.	n.d.	n.d.	n.d.	n.d.	n.d.	n.d.	n.d.	n.d.	n.d.	300	n.d.	n.d.	n.d.	n.d.	0.6	n.d.	n.d.
Summer Lake 2	N 42.725 W 120.647	1303	43	8.5	6.9	391	0.1	43	5	3	0.01	416	285	1.4	2.2	32	110	n.d.	−13.6	−120
MSH10-02	N 46.21 W 122.19	1520	n.d.	n.d.	n.d.	n.d.	n.d.	n.d.	n.d.	n.d.	n.d.	n.d.	250	n.d.	n.d.	n.d.	n.d.	1.3	n.d.	n.d.
MSH10-04	N 46.21 W 122.19	1520	n.d.	n.d.	n.d.	n.d.	n.d.	n.d.	n.d.	n.d.	n.d.	n.d.	250	n.d.	n.d.	n.d.	n.d.	0.2	n.d.	n.d.
Paradise Spring	N 46.803 W 121.719	1930	22.4	6.3	n.d.	n.d.	n.d.	n.d.	n.d.	n.d.	n.d.	n.d.	64	n.d.	n.d.	n.d.	n.d.	0.8	n.d.	n.d.

Table 1 (*continued*)

Spring name	Location	Elevation (m)	T (°C)	pH	B	Na	Mg	Si	K	Ca	Fe	HCO_3[a]	Cl	Br	F	I	SO_4	$\delta^{37}Cl$[b]	$\delta^{18}O$	δD
Weberg	N 44.001 W 119.650	1490	42.5	6.7	17.7	707	8.3	40	39	38	0.09	1823	50	0.1	4.4	48	1	0.1	−14.6	−121
Carbonate Spring	N 46.253 W 122.221	950	18.1	6.7	n.d.	n.d.	n.d.	n.d.	n.d.	n.d.	n.d.	n.d.	50	n.d.	n.d.	n.d.	n.d.	0.6	n.d.	n.d.
Olene	N 42.173 W 121.619	1255	39.5	7.9	0.5	100	2	33	5	25	0.06	53	35	n.d.	n.d.	n.d.	n.d.	0.9	−11.6	−103
SS McCloud	N 41.227 W 122.139	930	9.3	6.0	n.d.	n.d.	n.d.	n.d.	n.d.	n.d.	n.d.	n.d.	29	0.1	0.1	n.d.	n.d.	0.8	n.d.	n.d.
Klickitat	N 45.823 W 121.117	148	25.4	5.8	0.1	67	110	74	11	133	14.51	1096	21	n.d.	n.d.	n.d.	n.d.	1.1	−15.3	−114
Bagby	N 44.935 W 122.173	714	53.8	9.0	0.1	52	0.1	36	1	4	0.44	67	18	n.d.	n.d.	n.d.	n.d.	1.1	−12.8	−92
Minnehaha	N 43.075 W 122.276	1340	9.3	6.4	n.d.	n.d.	n.d.	n.d.	n.d.	n.d.	n.d.	n.d.	13	< 0.1	< 0.1	n.d.	n.d.	0.3	n.d.	n.d.
Sphynx	N 44.081 W 121.847	1560	4.9	8.5	n.d.	n.d.	n.d.	n.d.	n.d.	n.d.	n.d.	n.d.	10	< 0.1	0.2	n.d.	n.d.	−0.1, 0.0	n.d.	n.d.
Sulphur Creek	N 48.707 W 121.816	1035	6.2	5.1	n.d.	n.d.	n.d.	n.d.	n.d.	n.d.	n.d.	n.d.	6	n.d.	n.d.	n.d.	n.d.	0.6	n.d.	n.d.

(n.d.) not determined.

[a] Total alkalinity reported as bicarbonate.

Italicized samples contain <50 mg/mL Cl and are not further considered in discussion.

[b] Multiple values indicate replicate analyses.

Table 2
Select chemical data for the 9 Columbia Transect lavas.

Sample	Group	Coordinates	Region	Cl[a]	Br[b]	F[a]	I[b]	Cl/Nb	Cl/Zr	Ba/Nb	δ^{37}Cl
V457	2	N 46.098 W 122.342	Forearc	16.76	78.2	600	92	2.32	0.113	76.66	0
V348	2	N 46.063 W 122.431	Forearc	81.46	131	144	99	15.14	0.708	35.13	n.d.
L00-10	2	N 45.54 W 122.56	Portland Basin	65.93	152	317	26	7.89	0.401	43.01	0.6
L01-17	1	N 46.21 W 122.25	Mt. St. Helens	141.2	265	136	18	7.02	0.931	13.3	0.5
L01-25	1	N 46.06 W 121.33	Mt. Adams	139.6	222	156	27	11.54	1.02	19.41	−0.1
L01-24	1	N 45.97 W 121.39	Mt. Adams	156.7	308	197	28	12.38	1.045	19.39	0.7
L83-91	1	N 45.908 W 121.71	Backarc	18.79	54.7	164	22	0.56	0.096	12.42	0.5
L83-57	1	N 46.01 W 121.15	Backarc	64.71	58.5	75.1	21	7.92	0.605	12.48	0.1
SH-33	NA	N 46.22 W 122.19	Mt. St. Helens	119.1	244	121	16	24.21	0.993	58.33	0.8

Halogen concentrations and chlorine isotope data are from this study. Nb, Zr, and Ba data from Leeman et al. (2004, 2005).
[a] Concentration in ppm.
[b] Concentration in ppb.
NA (not applicable).
n.d. (not determined).

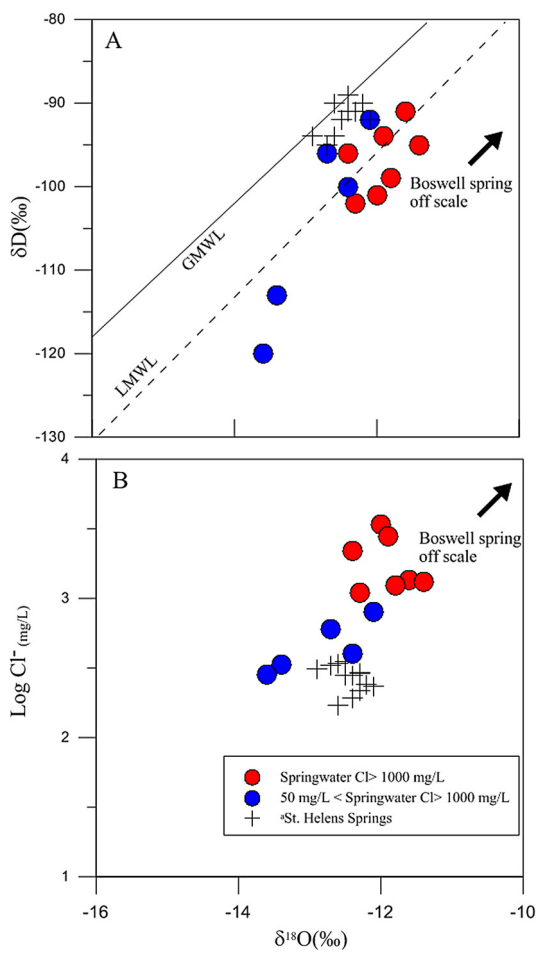

Fig. 3. A) δ^{18}O vs. δD values of the thermal and mineral springs. The global meteoric water line (GMWL, solid line; Craig, 1961) and calculated local meteoric water line (LMWL, dashed line; Bowen and Revenaugh, 2003), are shown for comparison. B) δ^{18}O value vs. log Cl concentration (mg/L) of the spring waters. [a]St. Helens spring data from Bergfeld et al. (2008).

weathering or alteration. The basalts were subdivided into two distinct compositional groups (Leeman et al., 2004, 2005) (Fig. 1; Table 2). Group 1 lavas chemically resemble intraplate basalts in that they exhibit smooth primitive mantle-normalized trace element profiles with no significant depletion of high field strength elements (HFSE; e.g., Ta, Nb) and trivial inputs of slab derived fluids as indicated by low Ba/Nb ratios (<20). Locations of Group 1 lavas range from the volcanic front to the backarc (Fig. 1). Group 2 basalts are calc-alkalic, exhibit Nb and Ta depletion relative to other incompatible trace elements, and have elevated Ba/Nb ratios (>20), all indicative of input of slab-derived fluids into their source region. The analyzed Group 2 basalts are located in the forearc region (Fig. 1), albeit similar lavas are distributed cross the arc.

Cl concentrations in the basalts are highest at the volcanic front (140–157 ppm) compared to the forearc (17–82 ppm) and the backarc (19–65 ppm). Cl/Nb and Cl/Zr ratios show similar crossarc trends with high values in arc front basalts compared to forearc and backarc basalts (Table 2). Br concentrations show a similar trend to Cl, with the highest concentrations at the volcanic arc front. In contrast, F concentrations are highest in the forearc (144–600 ppm), decreasing to 136–197 ppm at the volcanic front and 75–164 ppm in the backarc. Similar to F, I concentrations are highest in the forearc (26 to 99 ppb) and decrease at the volcanic front and backarc (<30 ppb) (Fig. 2c). I/Br and F/Br ratios also decrease from the forearc to the backarc. However, these bulk rock concentrations may have been modified due to variable degassing (see Section 5.3). δ^{37}Cl values range from −0.1‰ to +0.8‰ with no systematic cross-arc dependence. For example, the two samples from near Mt. Adams have δ^{37}Cl values of −0.1‰ and +0.7‰. Moreover, there is no significant correlation of δ^{37}Cl values with Cl concentration or its ratio to refractory incompatible elements (e.g., Cl/Nb, Cl/Zr).

The Mount St. Helens dacite sample has halogen contents and δ^{37}Cl values similar to those in the associated basalt from this volcano. Thus, it appears that the data presented here can be taken as broadly representative of the compositional spectrum for fresh Cascades volcanic rocks.

5. Discussion

5.1. Minimal contribution of seawater and sedimentary chlorine

Oxygen and hydrogen isotope data indicate a local meteoric water source for the springs (Fig. 3A), in agreement with previous studies (e.g., Hurwitz et al., 2005). Seawater (19,350 mg/L Cl) absorbed on sediments, and later extracted from them and diluted by

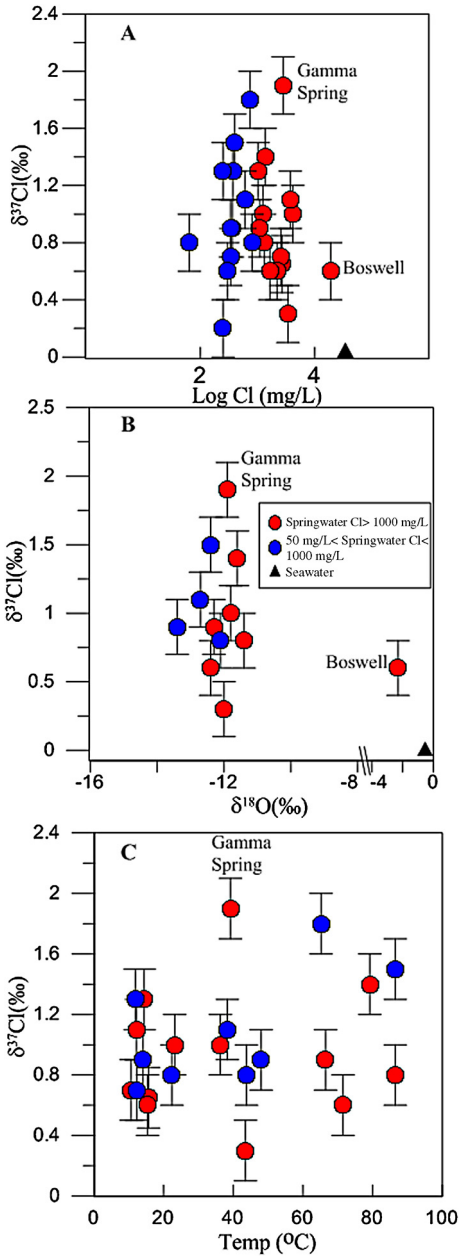

Fig. 4. δ^{37}Cl values of the spring waters as a function of A) log Cl concentration, B) δ^{18}O values and C) discharge temperature. Seawater (triangle) plotted for reference in panels A and B.

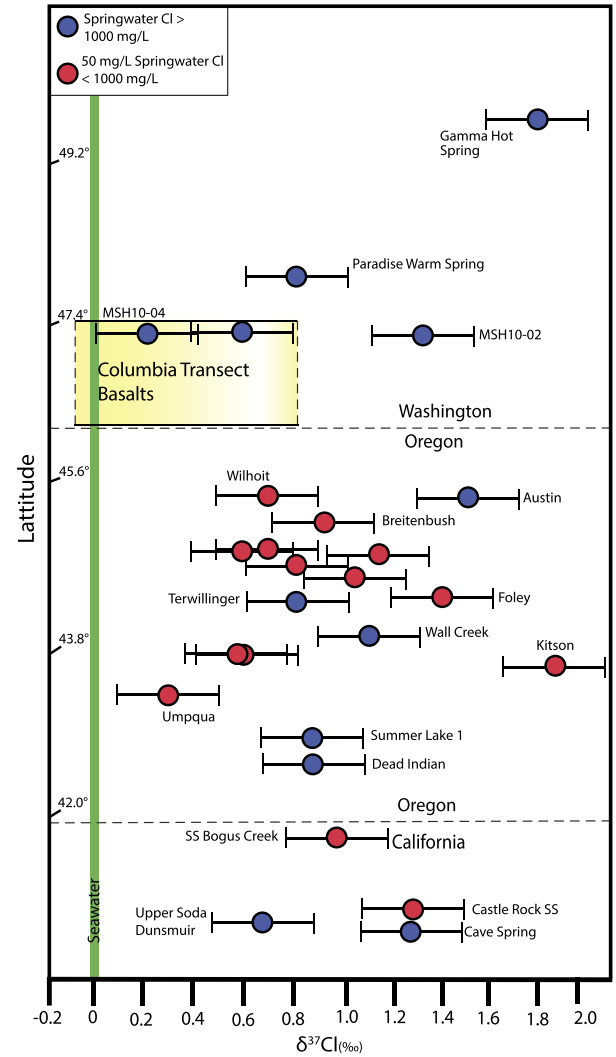

Fig. 5. Variation in δ^{37}Cl values of thermal springs along the Cascade Range. Blue and red dots represent Cl concentrations ranging between 50–1000 mg/L and ≥1000 mg/L, respectively. Yellow shaded region shows the range in δ^{37}Cl values of the 9 Columbia transect lavas. (For interpretation of the references to color in this figure legend, the reader is referred to the web version of this article.)

circulating meteoric water, potentially could account for elevated Cl content of many spring waters. However, seawater has a δ^{37}Cl value of 0‰ (Kaufmann et al., 1984), whereas all the spring waters have positive δ^{37}Cl values, thus suggesting there must be a significant non-seawater component of Cl. Cl/Br ratios of the springs are significantly higher than that of seawater (Fig. 6A), suggesting that if modified seawater trapped in sediments is a major source, then it either requires a major Br sink and/or Cl source. Additionally, marine aerosols are likely to contribute insignificant Cl to the thermal waters considering the low concentration of Cl (<1 mg/L) in rainwater from Central Oregon (Ingebritsen et al., 1994).

Underlying Eocene marine sediments of the Western Cascades and Lassen region have been considered to be major sources of Cl in local springs (Mariner et al., 2003; Mariner et al., 2006). Although the δ^{37}Cl values of sediments and (meta-)sedimentary rocks have a large range from ∼−3‰ to ∼+2‰, the vast majority of non-evaporite marine sediments have negative δ^{37}Cl values (e.g., Arcuri and Brimhall, 2003; Barnes et al., 2009; Selverstone and Sharp, 2013, 2015). Therefore, interaction between meteoric water and marine sediments is likely to shift waters to negative δ^{37}Cl values, as opposed to the positive δ^{37}Cl values observed.

5.2. Groundwater interaction with volcanic rocks

A potentially significant component to the analyzed spring waters is groundwater that has percolated through volcanic strata. Thus, fluid–rock interaction may contribute to dissolved solutes in the waters. Loose correlation between Cl concentrations and δ^{18}O values (Fig. 3B) suggests that Cl in spring waters could be derived from fluid–rock interaction. Moreover, conservative element ratios in many of the spring waters are similar to such ratios in the analyzed volcanic rocks. Molar Cl/Br ratios (483–2492; mean = 1220) of the analyzed Cascade Range lavas, overlap with the ratios observed in the spring waters (445–2734; mean = 967) (Fig. 6A). Molar Cl/B ratios of the spring waters (13–852; mean = 106) (Fig. 6B) partially overlap molar Cl/B ratios of the analyzed Columbia transect lavas (0.6–14.3; mean = 6.9), however higher Cl in most spring waters compared to the lavas suggests an ad-

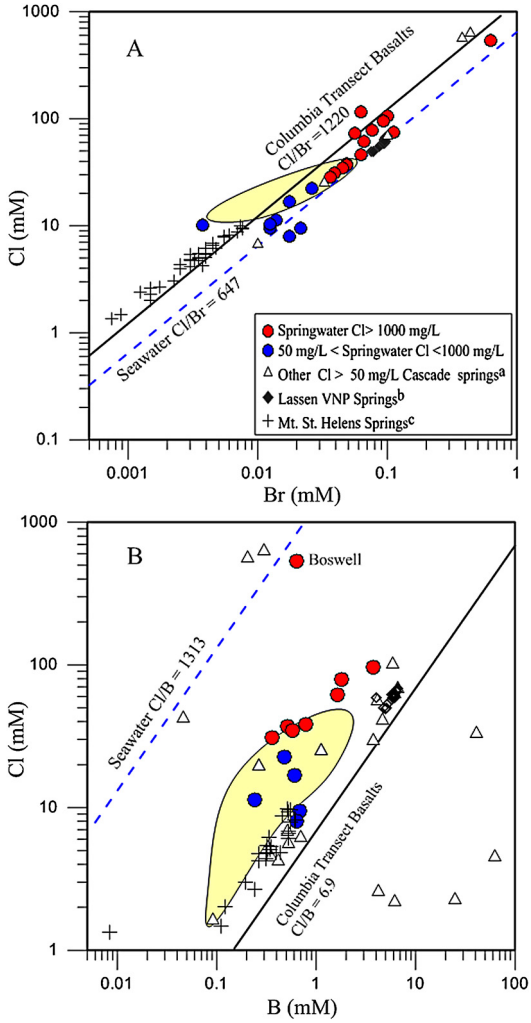

Fig. 6. Cl vs. A) Br concentration and B) B concentration of thermal waters. Dashed line = Seawater ratios of Cl/Br and Cl/B, respectively. Solid line = average ratios from Columbia Transect Lavas. [a]Data from Mariner et al. (1990, 1993, 2003). [b]Data from Thompson (1985). [c]Data from Bergfeld et al. (2008) and White (1963). Yellow fields denote Mt. St. Helens dome fumarole condensates from Shevenell and Goff (1993) ($n = 7$). (For interpretation of the references to color in this figure legend, the reader is referred to the web version of this article.)

ditional source of Cl (see Section 5.3). Mass balance calculations based on assumptions of Cl concentration in the volcanic rocks and magma production rates also suggest that leaching of Cl from volcanic rock is unlikely to be the major Cl source to the springs (e.g., Hurwitz et al., 2005). To further evaluate the effect of fluid–rock interaction on the Cl isotope composition of Cascade Range spring waters, we used an isotope mass balance model (e.g, Pennisi et al., 2000). In this model, we assume that successive volumes of water infiltrate a volume of rock and approach chemical equilibrium. The chemical composition of the water can be calculated as a function of the water–rock ratio (W/R), the distribution coefficient (which is the final concentration ratio of the element of interest in the rock versus that in water (C^f_{rock}/C^f_{water})), the isotope fractionation factor at a given temperature ($\Delta_{rock\text{-}water}$), and the initial isotope composition of the water ($\delta_{water,\ initial}$) and rock ($\delta_{rock,\ initial}$). We model meteoric water interacting with basalts and with underlying altered basalt (e.g., altered oceanic crust from accreted terranes) (Fig. 7). Interaction with marine sedimentary rocks was not considered as marine sediments have negative δ^{37}Cl values and cannot account for the positive δ^{37}Cl values of the spring waters. Previous work suggests that water–rock ratios for hot springs in the Cascade Range are 3 ± 1 (Ingebritsen et al., 1991). It is assumed that meteoric water has an initial Cl concentration of 3 mg/L and a δ^{37}Cl value of 0‰. Varying the Cl concentration of the meteoric water between 1 and 5 ppm makes essentially no difference in the models. Cl isotope fractionation factors between silicate minerals and fluids are very poorly constrained. Theoretical calculations predict that silicate minerals will have higher δ^{37}Cl values compared to co-existing brine by about +2 to +3‰ at room temperature (Schauble et al., 2003). In the models we use a $\Delta_{rock\text{-}water}$ of 0.5‰, based on extrapolation to a higher temperature (~300 °C). Lowering the temperature of interaction would increase the $\Delta_{rock\text{-}water}$ value, and hence could partly account for higher δ^{37}Cl values of the water assuming Cl exchange at lower temperatures. The host volcanic strata are modeled using an initial Cl concentration of 89 ppm and a δ^{37}Cl value of +0.4‰ (i.e., average values for volcanic rocks reported in this study). Interaction with amphibole-bearing altered oceanic crust was modeled using an initial Cl concentration of 207 ppm and a δ^{37}Cl value of +1.2‰ (Barnes and Cisneros, 2012). The distribution coefficient for Cl between aqueous fluid and silicate rock is not well determined, but in general Cl preferentially partitions into the aqueous phase. For example, Fabbrizio et al. (2013) report a D_{Cl} value between amphibole and fluid of ~0.005 at 2 GPa and between 900 and 1300 °C. Here we use higher D_{Cl} values (0.05 and 0.1) between rock and water considering the lower temperature of interaction; lower D values shift the modeled Cl concentration of the spring waters to higher values. Using these model parameters, it appears that the interaction of meteoric water with Cascades volcanic rocks cannot account for δ^{37}Cl values greater than about +1‰ and Cl concentrations greater than 2000 mg/L (Fig. 7). To account for more positive δ^{37}Cl values (> +1‰) in the fluids, interaction with rocks that have higher δ^{37}Cl values likely is required (e.g., altered volcanic rocks at depth).

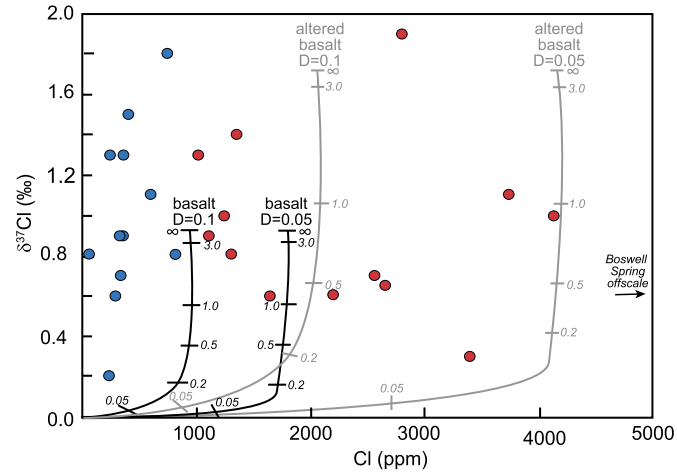

Fig. 7. δ^{37}Cl values vs. Cl concentration (mg/L) of spring waters. Red and blue symbols as in Figs. 3–6. Black and gray lines show modeled compositions of spring fluids with varying W/R ratios (tick marks on the lines) for meteoric water interaction with host basalts (black lines) or underlying altered basalt (gray lines), respectively. Assumed modeling parameters: meteoric water ($C^i = 3$ mg/L; $\delta^{37}Cl_{initial} = 0$‰); $\Delta_{rock\text{-}water} = 0.5$‰ ($T \approx 300$ °C) (poorly constrained; extrapolated from Schauble et al. (2003)); basalts ($C^i = 89$ ppm; $\delta^{37}Cl_{initial} = +0.4$‰; this study); altered oceanic crust ($C^i = 207$ ppm; $\delta^{37}Cl_{initial} = +1.2$‰) (Barnes and Cisneros, 2012); $D_{Cl} = 0.05$ and 0.1 (poorly constrained; extrapolated from Fabbrizio et al. (2013)). (For interpretation of the references to color in this figure legend, the reader is referred to the web version of this article.)

5.3. Degassing of chlorine and implications for magmatic processes

An additional possible source of Cl to the Cascade spring waters is via magmatic degassing. Previous work on Cl and I radioisotopes has suggested magmatic degassing contributes a large

portion of halogens to the thermal springs (Hurwitz et al., 2005). Melt inclusions from Cascade lavas have significantly higher Cl concentrations (up to ∼2600 ppm) (e.g., Le Voyer et al., 2010; Ruscitto et al., 2011) than the whole-rock basalts (average = 89 ppm; this study). Olivine-hosted melt inclusions from primitive Mt. Shasta basalts have elevated Cl/B ratios (5 to 900; average = 120; $n = 25$) (Le Voyer et al., 2010), overlapping the Cl/B ratios of the spring waters and higher than the bulk basalts (Fig. 6B). All of these observations imply shallow losses of Cl from Cascades magmas, probably as HCl component in magmatic gases; this is consistent with spectroscopic measurements of HCl outputs from Mt. St. Helens (Edmonds et al., 2008) and observations in other volcanic arcs (Shinohara, 2009).

The incorporation of HCl magmatic vapors into spring waters can also explain the elevated ($> \sim 1‰$) δ^{37}Cl values seen in many of these samples. Equilibrium chlorine isotopic fractionation during magmatic degassing is likely negligible (Barnes et al., 2014; Rizzo et al., 2013; Schauble et al., 2003); however, significant kinetic fractionation has been documented in high-temperature (>100 °C) fumarole gases (δ^{37}Cl values $> +10‰$) and has been reproduced experimentally (Sharp et al., 2010). High δ^{37}Cl values can result from open-system (Rayleigh) distillation during near surface loss of ^{35}Cl to an aqueous fluid phase such that ^{37}Cl is subsequently enriched in residual gaseous HCl (Sharp et al., 2010). The equilibrium chlorine isotope fractionation between HCl gas and Cl^- is $\sim +1.5‰$ between 50 and 100 °C (Schauble et al., 2003), therefore even small amounts of degassing can explain the high δ^{37}Cl values observed in the thermal springs. Symonds et al. (2003) also propose a two-step "scrubbing" process within Cascade arc volcanoes by which HCl is removed by deep thermal water (150–350 °C) and then by shallow meteoric water. It is conceivable that the exsolved HCl progressively fractionates as ^{35}Cl is preferentially "scrubbed out" in the deeper reservoirs and eventually the ^{37}Cl-enriched vapor mixes with the shallow ground-waters.

Recent studies in other arc settings have also used Cl isotope data to argue for contributions of magmatic Cl to thermal springs. Spring waters from the Lesser Antilles have δ^{37}Cl values between $-0.65‰$ and $+0.12‰$ (Li et al., 2015). These values are interpreted to reflect an inferred slightly negative δ^{37}Cl value for the upper mantle owing to contribution of slab-derived Cl, without any isotopic modification due to limited HCl degassing (Li et al., 2015). Thermal springs from the Taupo Volcanic Zone have δ^{37}Cl values (ranging from $-0.8‰$ to $+0.7‰$) that are also interpreted to reflect contribution of magmatic Cl, albeit with modification due to isotopic fractionation (Bernal et al., 2014). Therefore, if thermal springs indeed sample magmatic Cl, either directly from influx of magmatic gases or indirectly via leaching of volcanic strata, they provide a means of characterizing the general nature of the magmatic component in volcanic arcs.

6. Conclusions

In this study, we use the major/minor element concentrations and chlorine stable isotope compositions of thermal and mineral springs along the Cascade Range in order to provide constraints on the chlorine sources. Major findings include the following:

1) Cascade spring waters typically have Cl/Br ratios slightly higher than seawater, Cl/B ratios significantly lower than seawater, and positive δ^{37}Cl values. These observations are inconsistent with significant contributions of marine Cl in the form of seaspray or connate waters to the spring waters.

2) Halogens concentrations and Cl/Br and Cl/B ratios in spring waters can reasonably be explained by hydrothermal interaction between meteoric water and volcanic rocks similar in composition to analyzed Cascade basalts (and dacite). However, isotope mass balance modelling shows that water interaction with fresh lavas cannot account for the full range of Cl concentrations and δ^{37}Cl values observed in the springs.

3) The highest δ^{37}Cl values ($> +1‰$) of the spring waters seemingly require additional conditions or processes. One possible explanation is that such waters interacted with rocks having higher δ^{37}Cl values than the analyzed fresh lavas, perhaps via percolation through altered volcanic rocks at depth. An alternate explanation is that such waters incorporated ^{37}Cl-enriched HCl vapor exsolved from cooling magmas.

We conclude that thermal spring waters appear to provide a reasonable proxy for the Cl isotope compositions of associated volcanic rocks in the Cascades, albeit the origin of the most elevated δ^{37}Cl values ($> +1‰$) remains uncertain. Future work on the Cl isotope composition of fumarole gases and melt inclusions in the Cascade Range might provide insights into Cl behavior during magmatic processes, and help to further assess Cl isotope fractionation during degassing. Quantification of the magmatic component in thermal springs is necessary to fully understand global volatile cycling through subduction zones.

Acknowledgements

This paper is part of the M.S. thesis of the first author. We thank T. Larson for help with oxygen and hydrogen isotope analyses, J. Lewicki and D. Bergfeld for providing spring samples, E. Santillan and M. Cisneros for their assistance in the field, C. Kusebauch for bulk rock halogen analyses, M. Huebner, J. Fitzpatrick, and L. Clor for help with geochemical analyses, and the Jackson School of Geosciences for funding and support. S. Hurwitz was funded by the U.S. Geological Survey, Volcano Hazards Program. Comments by B. McCleskey, two anonymous reviewers, and editor T. Mather helped to improve this work.

References

Arcuri, T., Brimhall, G., 2003. The chloride source for atacamite mineralization at the Radomiro Tomic porphyry copper deposit, northern Chile. Econ. Geol. 98, 1667–1681.

Barnes, J.D., Cisneros, M., 2012. Mineralogical control on the chlorine isotope composition of altered oceanic crust. Chem. Geol. 326–327, 51–60.

Barnes, J.D., Stefansson, A., 2012. Chlorine isotope geochemistry of Icelandic geothermal waters. Mineral. Mag. 76, 1456.

Barnes, J.D., Sharp, Z.D., Fischer, T.P., 2008. Chlorine isotope variations across the Izu–Bonin–Mariana arc. Geology 36, 883–886.

Barnes, J.D., Sharp, Z.D., Fischer, T.P., Hilton, D.R., Carr, M.J., 2009. Chlorine isotope variations along the Central American volcanic front and back arc. Geochem. Geophys. Geosyst. 10, Q11S17. http://dx.doi.org/10.1029/2009GC002587.

Barnes, J., Prather, T., Cisneros, M., Befus, K., Gardner, J., Larson, T., 2014. Stable chlorine isotope behavior during volcanic degassing of H_2O and CO_2 at Mono Craters, CA. Bull. Volcanol. 76, 1–13.

Bebout, G.E., 2007. Trace element and isotopic fluxes/subducted slab. In: Heinrich, D.H., Karl, K.T. (Eds.), Treatise on Geochemistry. Pergamon, Oxford, pp. 1–50.

Bergfeld, D., Evans, W.C., McGee, K., Spicer, K.R., 2008. In: Sherrod, David R., Scott, William E., Stauffer, Peter H. (Eds.), A Volcano Rekindled: The Renewed Eruption of Mount St. Helens, 2004–2006. In: Geological Survey Professional Paper, vol. 1750.

Bernal, N.F., Gleeson, S.A., Dean, A.S., Liu, X.-M., Hoskin, P., 2014. The source of halogens in geothermal fluids from the Taupo Volcanic Zone, North Island, New Zealand. Geochim. Cosmochim. Acta 126, 265–283.

Bostock, M., Hyndman, R., Rondenay, S., Peacock, S., 2002. An inverted continental Moho and serpentinization of the forearc mantle. Nature 417, 536–538.

Bowen, G.J., Revenaugh, J., 2003. Interpolating the isotopic composition of modern meteoric precipitation. Water Resour. Res. 39, 1299.

Brocher, T.M., Parsons, T., Tréhu, A.M., Snelson, C.M., Fisher, M.A., 2003. Seismic evidence for widespread serpentinized forearc upper mantle along the Cascadia margin. Geology 31, 267–270.

Chiaradia, M., Barnes, J.D., Cadet-Voisin, S., 2014. Chlorine stable isotope variations across the Quaternary volcanic arc of Ecuador. Earth Planet. Sci. Lett. 396, 22–33.

Craig, H., 1961. Isotopic variations in meteoric waters. Science 133 (3465), 1702–1703.

Edmonds, M., McGee, K.A., Doukas, M.P., 2008. Chlorine degassing during the lava dome-building eruption of Mount St. Helens. 2004–2005. In: U.S. Geological Survey Professional Paper, vol. 1750, pp. 573–589.

Eggenkamp, H.G.M., 1994. The Geochemistry of Chlorine Isotopes. Universiteit Utrecht, p. 151.
Evans, W.C., van Soest, M.C., Mariner, R.H., Hurwitz, S., Ingebritsen, S.E., Wicks, C.W., Schmidt, M.E., 2004. Magmatic intrusion west of Three Sisters, central Oregon, USA: the perspective from spring geochemistry. Geology 32, 69–72.
Fabbrizio, A., Stalder, R., Hametner, K., Günther, D., Marquardt, K., 2013. Experimental partitioning of halogens and other trace elements between olivine, pyroxenes, amphibole and aqueous fluid at 2 GPa and 900–1300 °C. Contrib. Mineral. Petrol. 166, 639–653.
Fehn, U., 2012. Tracing crustal fluids: applications of natural ^{129}I and ^{36}Cl. Annu. Rev. Earth Planet. Sci. 40, 45–67.
Hildreth, W., 2007. Quaternary magmatism in the Cascades – geologic perspectives. In: U.S. Geological Survey Professional Paper, vol. 1744, pp. 1–125.
Hurwitz, S., Mariner, R.H., Fehn, U., Snyder, G.T., 2005. Systematics of halogen elements and their radioisotopes in thermal springs of the Cascade Range, Central Oregon, Western USA. Earth Planet. Sci. Lett. 235, 700–714.
Ingebritsen, S., Sherrod, D., Mariner, R., 1989. Heat flow and hydrothermal circulation in the Cascade Range, north-central Oregon. Science 243, 1458–1462.
Ingebritsen, S.E., Mariner, R.H., Sherrod, D.R., 1991. Hydrothermal systems of the Cascade Range, north-central Oregon. In: U.S. Geological Survey Open File Report, vol. 91-69. 217 pp.
Ingebritsen, S.E., Mariner, R.H., Sherrod, D.R., 1994. Hydrothermal systems of the Cascade Range, north-central Oregon. In: U.S. Geological Survey Professional Paper, vol. 1044L, pp. 807–812.
James, E.R., Manga, M., Rose, T.P., 1999. CO_2 degassing in the Oregon Cascades. Geology 27 (9), 823–826.
Kaufmann, R., Long, A., Bentley, H., Davis, S., 1984. Natural chlorine isotope variations. Nature 309, 338–340.
Kendrick, M.A., Woodhead, J.D., Kamenetsky, V.S., 2012. Tracking halogens through the subduction cycle. Geology 40, 1075–1078.
Le Voyer, M., Rose-Koga, E.F., Shimizu, N., Grove, T.L., Schiano, P., 2010. Two contrasting H_2O-rich components in primary melt inclusions from Mount Shasta. J. Petrol. 51, 1571–1595.
Leeman, W.P., Tonarini, S., Chan, L.H., Borg, L.E., 2004. Boron and lithium isotopic variations in a hot subduction zone – the southern Washington Cascades. Chem. Geol. 212, 101–124.
Leeman, W.P., Lewis, J.F., Evarts, R.C., Conrey, R.M., Streck, M.J., 2005. Petrologic constraints on the thermal structure of the Cascades arc. J. Volcanol. Geotherm. Res. 140, 67–105.
Li, L., Bonifacie, M., Aubaud, C., Crispi, O., Dessert, C., Agrinier, P., 2015. Chlorine isotopes of thermal springs in arc volcanoes for tracing shallow magmatic activity. Earth Planet. Sci. Lett. 413, 101–110.
Manning, C.E., 2004. The chemistry of subduction-zone fluids. Earth Planet. Sci. Lett. 223, 1–16.
Mariner, R., Presser, T., Evans, W., Pringle, M., 1990. Discharge rates of fluid and heat by thermal springs of the Cascade Range, Washington, Oregon, and northern California. J. Geophys. Res. 95, 19517–19531.
Mariner, R.H., Presser, T.S., Evans, William C., 1993. Geothermometry and water–rock interaction in selected thermal systems in the cascade range and modoc plateau, western United States. Geothermics 22 (1), 1–15.
Mariner, R.H., Evans, W.C., Presser, T.S., White, L.D., 2003. Excess nitrogen in selected thermal and mineral springs of the Cascade Range in northern California, Oregon, and Washington: sedimentary or volcanic in origin? J. Volcanol. Geotherm. Res. 121, 99–114.
Mariner, R.H., Venezky, D.Y., Hurwitz, S., 2006. Chemical and isotopic database of water and gas from hydrothermal systems with an emphasis for the western United States. In: U.S. Geological Survey Digital Data Series, vol. 169. http://pubs.usgs.gov/ds/2005/169/.
McCrory, P.A., Blair, J.L., Oppenheimer, D.H., Walter, S.R., 2004. Depth to the Juan de Fuca slab beneath the Cascadia subduction margin: a 3-D model for sorting earthquakes. In: US Department of the Interior. In: U.S. Geological Survey Data Series, vol. 91. http://pubs.usgs.gov/ds/91/.
Pennisi, M., Leeman, W.P., Tonarini, S., Pennisi, A., Nabelek, P.I., 2000. Boron, Sr, O, and H isotope geochemistry of groundwaters from Mt. Etna (Sicily) – hydrologic implications. Geochim. Cosmochim. Acta 64, 961–974.
Rizzo, A.L., Caracausi, A., Liotta, M., Paonita, A., Barnes, J.D., Corsaro, R.A., Martelli, M., 2013. Chlorine isotope composition of volcanic gases and rocks at Mount Etna (Italy) and inferences on the local mantle source. Earth Planet. Sci. Lett. 371–372, 134–142.
Ruscitto, D.M., Wallace, P.J., Kent, A.J.R., 2011. Revisiting the compositions and volatile contents of olivine-hosted melt inclusions from the Mount Shasta region: implications for the formation of high-Mg andesites. Contrib. Mineral. Petrol. 162, 109–132.
Schauble, E.A., Rossman, G.R., Taylor, H., 2003. Theoretical estimates of equilibrium chlorine-isotope fractionations. Geochim. Cosmochim. Acta 67, 3267–3281.
Schmidt, M.E., Grunder, A.L., Rowe, M.C., 2008. Segmentation of the Cascade Arc as indicated by Sr and Nd isotopic variation among diverse primitive basalts. Earth Planet. Sci. Lett. 266, 166–181.
Schnetger, B., Muramatsu, Y., 1996. Determination of halogens, with special reference to iodine, in geological and biological samples using pyrohydrolysis for preparation and inductively coupled plasma mass spectrometry and ion chromatography for measurement. Analyst 121, 1627–1631.
Selverstone, J., Sharp, Z.D., 2013. Chlorine isotope constraints on fluid–rock interactions during subduction and exhumation of the Zermatt–Saas ophiolite. Geochem. Geophys. Geosyst. 14, 4370–4391. http://dx.doi.org/10.1002/ggge.20269.
Selverstone, J., Sharp, Z.D., 2015. Chlorine isotope behavior during prograde metamorphism of sedimentary rocks. Earth Planet. Sci. Lett. 417, 120–131.
Sharp, Z., Barnes, J., Fischer, T., Halick, M., 2010. An experimental determination of chlorine isotope fractionation in acid systems and applications to volcanic fumaroles. Geochim. Cosmochim. Acta 74, 264–273.
Shevenell, L., Goff, F., 1993. Addition of magmatic volatiles into the hot spring waters of Loowit Canyon, Mount St. Helens, Washington, USA. Bull. Volcanol. 55, 489–503.
Shinohara, H., 2009. A missing link between volcanic degassing and experimental studies on chloride partitioning. Chem. Geol. 263, 51–59.
Straub, S.M., Layne, G.D., 2003. The systematics of chlorine, fluorine, and water in Izu arc front volcanic rocks: implications for volatile recycling in subduction zones. Geochim. Cosmochim. Acta 67 (21), 4179–4203.
Symonds, R.B., Janik, C.J., Evans, W.C., Ritchie, B.E., Counce, D., Poreda, R.J., Iven, M., 2003. Scrubbing masks magmatic degassing during repose at cascade-range and Aleutian-Arc Volcanoes. U.S. Geological Survey Open-File Report: 03-435.
Syracuse, E.M., van Keken, P.E., Abers, G.A., 2010. The global range of subduction zone thermal models. Phys. Earth Planet. Inter. 183, 73–90.
Thompson, J.M., 1985. Chemistry of thermal and nonthermal springs in the vicinity of Lassen Volcanic National Park. J. Volcanol. Geotherm. Res. 25 (1), 81–104.
van Keken, P.E., Hacker, B.R., Syracuse, E.M., Abers, G.A., 2011. Subduction factory: 4. Depth-dependent flux of H_2O from subducting slabs worldwide. J. Geophys. Res. 116, B01401. http://dx.doi.org/10.1029/2010JB007922.
Villemant, B., Boudon, G., 1999. H_2O and halogen (F, Cl, Br) behaviour during shallow magma degassing processes. Earth Planet. Sci. Lett. 168, 271–286.
Villemant, B., Hammouya, G., Michel, A., Semet, M.P., Komorowski, J.C., Boudon, G., Cheminée, J.L., 2005. The memory of volcanic waters: shallow magma degassing revealed by halogen monitoring in thermal springs of La Soufrière volcano (Guadeloupe, Lesser Antilles). Earth Planet. Sci. Lett. 237, 710–728.
Wells, R., Bukry, D., Friedman, R., Pyle, D., Duncan, R., Haeussler, P., Wooden, J., 2014. Geologic history of Siletzia, a large igneous province in the Oregon and Washington Coast Range: correlation to the geomagnetic polarity time scale and implications for a long-lived Yellowstone hotspot. Geosphere 10, 692–719.
White, D.E., 1963. Chemical Composition of Subsurface Waters: Tabulation and Discussion of Chemical Analyses. No. 440. US Government Printing Office.
Wilson, D.S., 1988. Tectonic history of the Juan de Fuca Ridge over the last 40 million years. J. Geophys. Res., Solid Earth (1978–2012) 93, 11863–11876.
Zhang, M., Hobbs, M.Y., Frape, S.K., Nordstrom, D.K., Ball, J.W., McCleskey, R.B., 2004. Stable chlorine isotopic composition of geothermal waters from Yellowstone National Park. In: Wanty, R.B., Seal, R.R. (Eds.), Water–Rock Interactions: Proceedings of the Eleventh International Symposium on Water–Rock Interaction, vol. 1, pp. 233–236.